Available online at www.sciencedirect.com

ScienceDirect

Procedia IUTAM 16 (2015) 115 – 122

Procedia IUTAM

www.elsevier.com/locate/procedia

IUTAM Symposium on Dynamics of Capsules, Vesicles and Cells in Flow

In Situ Encapsulation Kinetics monitored by Microfluidics

Ingmar Polenz,*[a] Quentin Brosseau,[a] Jean-Christophe Baret[a,b]

[a] *Max-Planck Institute for Dynamics and Self-organization, Am Fassberg 17, D-37077 Göttingen, Germany*
[b] *Centre de Recherche Paul Pascal, Université de Bordeaux, 115 Avene Schweitzer, F-33600 Pessac*

Abstract

We use microfluidic PDMS devices to monitor the encapsulation process occurring at an emulsion droplet interface which is indicated by the changes in the droplet interfacial deformability. Deformations are induced by constriction chambers at the microfluidic chip. This method allows for a precise measurement of *in situ* microencapsulation early kinetics (below 0.5 s). We study the formation of polyurea microcapsules (PUMCs). Shell formation occurs at the oil-water interface by an immediate reaction of a di- or multi amine dissolved in the aqueous phase and a diisocyanate dissolved in the oil phase. We are able to address the reactivity of certain reactants on the microencapsulation process. We observe that both monomers of this encapsulation contribute differently which is in contrast to the present understanding of the PUMC formation. In addition, we quantify the retarding effect of the interface stabilizing agent (surfactant) on the encapsulation kinetics. Our approach shows that microfluidics is efficient for monitoring and studying *in situ* encapsulations up to the potential for the determination of interfacial polymerization kinetics for the generation of microcapsules with well-defined properties and the study of soft reactive interfaces.

Peer-review under the responsibility of the organizing committee of DYNACAPS 2014 (Dynamics of Capsules, Vesicles and Cells in Flow).

Keywords: microfluidics, *in situ* encapsulation, polyurea, interfacial polymerization kinetics

1. Introduction

The utility of microcapsules for the programmable release and storage is of particular importance in agriculture, drug release, cosmetic and food industry as well as in textile and paper manufacturing.[1,2] *In situ* encapsulations (ISEs) that proceed *via* interfacial polymerizations are known since the 1960s and offer a facile route for the rapid production of solid shells along emulsion droplets for entrapping of both hydrophilic and hydrophobic ingredients under mild conditions of pressure and temperature.[3,4] Namely, the polymers polyurea, polyamide and polysiloxane are widely used for encapsulation due to their physicochemical properties.[2] However, common techniques applied to ISEs do not provide control over the capsule size and dispersity. To date, there is a lack of reliable quantitative

Peer-review under the responsibility of the organizing committee of DYNACAPS 2014 (Dynamics of Capsules, Vesicles and Cells in Flow).
doi:10.1016/j.piutam.2015.03.014

information on the encapsulation kinetics and understanding of the governing mechanisms that affect the shell formation which are prerequisites for the control of the final capsule properties.

In these proceedings, we report on a method for monitoring the dynamics of *in situ* encapsulations by means of microfluidics. We measure the deformability changes of water-in-oil (W/O) emulsion droplets while generating a polymeric shell at the interface by controlled interfacial deformations induced by hydrodynamic shear stresses in microfluidic constriction chambers. We investigate the polyurea microencapsulation; polyurea microcapsule (PUMC) formation occurs at the oil-water interface by immediate reaction of amines dissolved in the aqueous phase and isocyanates that are dissolved in the oil phase. By applying principles of polymerization kinetics we determine the polyurea encapsulation rate law. Reactivities of certain amine/isocyanate combinations are compared and the retardation of the encapsulation by the surfactant is quantified. Encapsulation early kinetics are accessible with our technique that are resolved in milliseconds and can be applied for a wide range of reactant concentrations (0.001–30 wt.%). The results reveal that our approach is valuable to gain deep insights into the mechanism of *in situ* encapsulations and it opens doors for the development of encapsulation processes yielding microcapsules with adjustable mechanical properties.

Nomenclature

ABIL	Abil® EM 90, surfactant for W/O emulsions composed of block-copolymers based on polysiloxanes and polyethers
AM	amine
BAS	BASONAT HI100, the HDI-isocyanurate
En	ethylenediamine
HDI	1,6-hexamethylene diisocyanate
HMDA	1,6-hexamethylenediamine
IC	isocyanate
ISE	*in situ* encapsulation
KMC	KMC 113 oil, an isomer mixture of 2,6 and 1,7-diisopropyl naphthalene
PDMS	polydimethylsiloxan
PEI	polyethyleneimine
PUMC	polyurea microcapsule
TDI	2,4-toluene diisocyanate
TEPA	tetraethylenepentamine
W/O	water-in-oil emulsion

2. Materials and Methods

We fabricate microfluidic polydimethylsiloxane (PDMS) devices by standard methods of soft lithography.[5] The wetting properties of our channels are controlled by hydrophobization of the walls with Aquapel®. The height of the channels is adjusted to 100 μm.

Amines 1,6-hexamethylenediamine (HMDA), ethylenediamine (En), tetraethylenepentamine (TEPA), polyethyleneimine (PEI, M_N = 600 g·mol^{-1}), as well as isocyanates 2,4-toluene diisocyanate (TDI) and 1,6-hexamethylene diisocyanate (HDI) are purchased from Sigma Aldrich and used as received. Surfactant Abil® Em 90 is purchased from Evonik Industries and the HDI isocyanurate Basonat® HI100 from BASF SE and were used as received. We use KMC 113 oil (Fischer Scientific, ρ = 0.89 g·cm^{-3}, η = 9.8 cP; $\gamma_{oil\text{-}water}$ = 37 mN·m^{-1}) as the isocyanate and surfactant dispersant which is an isomer mixture of 1,7- and 2,6-diisopropyl naphthalene, due to its solubility properties for the reactants and its non-swelling behavior towards PDMS. In general, interfacial polymerizations are step-growth polymerizations[6] that are characterized by a rapid conversion of the reactants. One of the reactants is dissolved in an aqueous phase and the second is dissolved in the oily fluid. As soon as long – and most-likely cross-linked – polymer chains are formed the network is precipitating at the water-oil interface to form a

solid stable shell. Each reactant and also oligomer acts as initiator for the formation of longer polymer chains. In our investigations we focus on the interfacial polyurea formation; an amine, dissolved in the aqueous phase, reacts with the isocyanate, dissolved in the oil, to form a polyurea network at the emulsion droplet interface. The reaction scheme of the polyurea formation and the structures of amines and isocyanates that are used in this work are depicted in Figure 1.

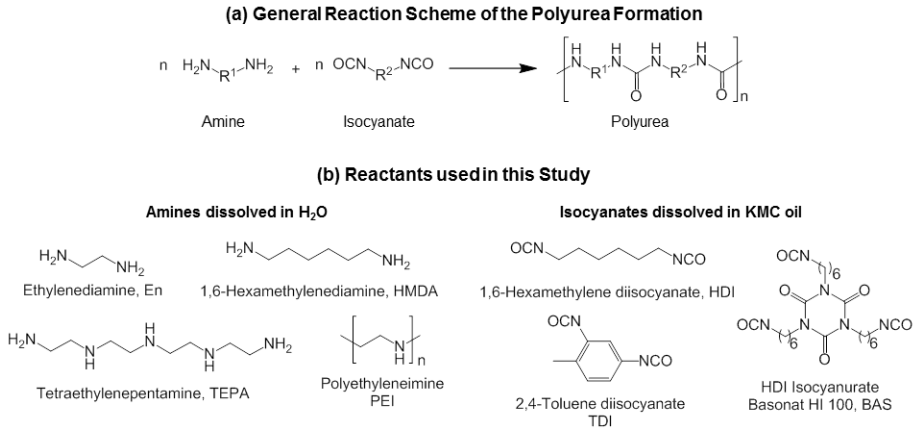

Fig. 1 (a) General reaction scheme of the polyurea microencapsulation and (b) reactants used in our investigations.

A general design of the microfluidic chip is depicted in Figure 2a. The emulsification and polyurea encapsulation are decoupled at the microfluidic chip to prevent an immediate clogging of the device by the rapid polymer formation. An aqueous amine solution ($5 \cdot 10^{-5}$ – 1 M) is emulsified in KMC oil at a flow-focusing T-junction. The emulsifier is either a pure KMC oil solution or contains the surfactant Abil® EM 90 ($2.2 \cdot 10^{-6}$ – $3.3 \cdot 10^{-4}$ M).

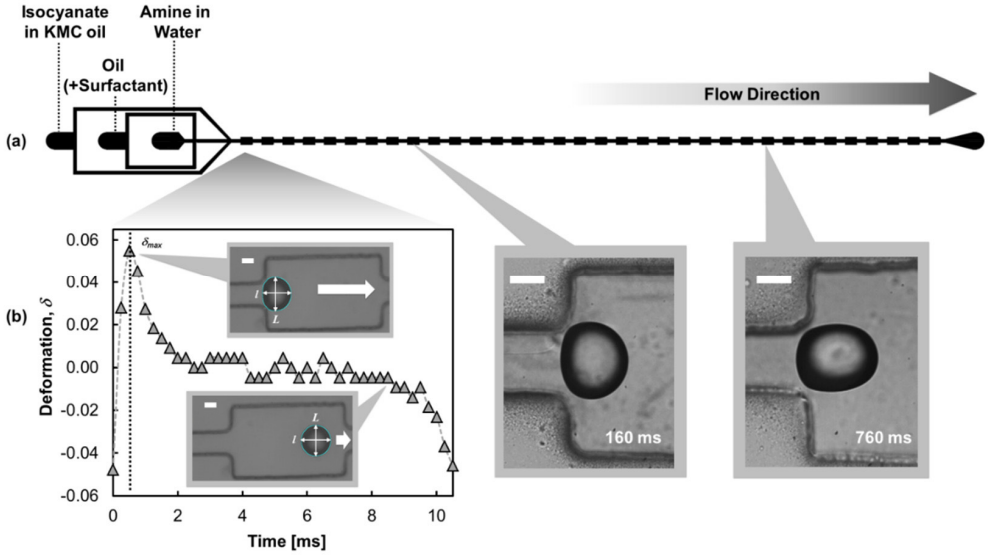

Fig. 2 (a) Device design for monitoring the encapsulation dynamics of interfacial polymerizations by measuring the deformability using microfluidic constriction chambers. (b) General readout: deformation profile of W/O emulsion droplets and deformability change over time while forming a polymeric shell at the interface. Multiple image processing is performed to detect the droplet contour over time. (Scale bar: 50 µm)

The water-in-oil (W/O) emulsion droplets are then flown into a V-junction where the isocyanate ($2.5 \cdot 10^{-3}$ – 1 M in KMC oil) is fed. In total, the device is run with three fluid flows and the flow rates of the aqueous phase, the emulsifier and the outer phase are held constant at 100, 2450 and 1050 $\mu L \cdot h^{-1}$.

3. Results and Discussion

Recently, we reported on a microfluidic dynamic tensiometer,[7] inspired by both the droplet deformation under shear, studied by Taylor in 1934 and a microfluidic tensiometer designed by Cabrel *et al.*.[8,9] We measured interfacial tensions in W/O emulsions at short time scales by analyzing the droplet deformation changes to study the surfactant adsorption dynamics at soft interfaces. Based on the principles of droplet deformations under hydrodynamic shear we designed a microfluidic chip to monitor interfacial polymerizations. The general design of the microfluidic device is shown in Figure 2a.

The reactants in our investigations differ in their reactivity and their latent ability to form branched or cross-linked networks.[10,11] With our method we want to address the reactant reactivity at the microencapsulation process and correlate these reactivities to the chemical structure. Monodisperse water-in-oil droplets are produced at a flow-focusing T-junction. An additional oil stream (see Fig. 2a) containing the isocyanate is fed to the emulsion *via* a V-junction. The droplets are then transversally deformed in a series of planar sudden expansions, linked by channels. The droplet deformation is recorded by high speed imaging (Phantom v311); the droplet contour is detected by a house made image processing software. In Figure 2b a general experimental readout for a single chamber is shown. The parameter that we measure is the dimensionless droplet deformation δ, which is defined by the droplet longitudinal l and transversal expansion L by

$$\delta = \frac{L - l}{L + l} \tag{1}$$

and proceeds as follows in our experiments: while entering the planar expansion the droplet deforms transversally to the flow direction and reaches a maximum (δ_{max}) before relaxing to a sphere ($\delta = 0$) and deforming longitudinally (δ decreases) when entering the outlet constriction. In the further text we use the maximum deformation δ_{max} as an indicator for the maximum tensile stress acting on the emulsion droplet interface.

In Figure 3a the maximum deformation δ_{max} as a function of the polymerization time (expansion chamber count) at amine concentration ranging between 0.001–0.5 wt.% are plotted.

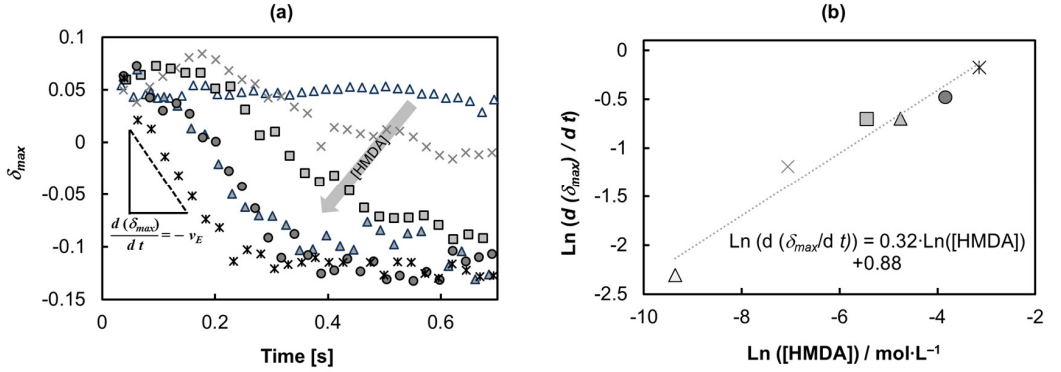

Fig. 3 (a) Maximum deformations δ_{max} as a function of the reaction time for the polymerizations using TDI / HMDA at HMDA concentrations ▲ 0.001 wt.%, x 0.01 wt.%, ■ 0.05 wt.%, ▲ 0.1 wt.%, ● 0.25 wt.%, x 0.5 wt.%. The TDI concentration is 2.5 wt.%. Exemplary, the value for d (δ_{max}) / dt for the HMDA concentration of 0.5 wt.% is elucidated by the dotted black line. Slopes are taken from the graph where the deformability loss over time is linear. (b) Double-logarithmic plot of d(δ_{max})/dt versus the amine concentration; the slope equals the order referring to the amine HMDA in the encapsulation rate equation that yields 0.32.

While forming a polymeric shell along the emulsion droplet we detect a decrease in δ_{max}. Visibly the droplet shape at δ_{max} changes dramatically as it is also shown in the micrograph images in Figure 2b. At the initial stage of the polymerization ($t = 0$) where no polymer film covers the droplet, the droplet deformation is purely dominated by the interfacial tension. With increasing monomer conversion a solid shell is forming at the W/O interface. As a consequence, the mechanical properties of the interface change dramatically and the deformation of the capsule is now dominated by the viscoelastic properties of the polymer film. The interfacial polymerization proceeds over the whole channel length even when the droplets are in a confined state. At increasing monomer conversion a rigidification of the W/O-interface proceeds due to the increasing polymer amount. As a consequence of the rigidification of the interface, the value of δ_{max} decreases along the microfluidic channel at higher expansion chamber counts (Fig. 2b and 3a). In this case the prolate deformation of the droplet induced by channel confinement is not relaxed anymore at the expansion. We observe in the last part of our channel that the value of δ_{max} reaches a plateau where our method is no longer appropriate for detection.

Accounting to basic principles of step growth polymerization kinetics,[6] the polymerization rate law for the polyaddition of an isocyanate IC and an amine AM reads

$$v_P = k_P \cdot [\mathrm{IC}]^a \cdot [\mathrm{AM}]^b \tag{2}$$

where v_P is the net polymerization rate, k_P the net polymerization rate constant and a, b the reaction orders of the isocyanate and the amine.

The stress T_1 required for an elastic transversal deformation of a spherical capsule having a membrane thickness h equals[12]

$$T_1 = 12 \cdot h \cdot \mathrm{E} \cdot \left(\frac{\lambda_1}{\lambda_2} - \frac{1}{\lambda_1^3 \cdot \lambda_2^3} \right) \cdot \left(1 + 0.1 \cdot \lambda_2^2 \right) \tag{3}$$

where E is Young`s modulus and λ_1 and λ_2 are the principal stretch ratios in meridional and circumferential directions that are in direct correlation to δ (see Briscoe *et al.* and Pozrikidis reference [12]). This relation is valid in the case of thin shells ($h << r$) which matches with our experimental conditions. At the early kinetics of the reactive encapsulation solely thin polymer films are formed along the W/O-droplet interface. We see that the transversal deformation basically is linked to the shell thickness and the elastic properties of the capsule. Thus, the changes in the shell thickness over time can be translated into monomer consumption and, therefore, also into polymerization kinetics. In this study we focus on the changes in the deformabilitiy of the interface at an interfacial polymerization. In a separate work we quantify the results by additional information on the shell thickness and gain the polymerization kinetics. In a first simple approach we correlate the deformability changes to the polyaddition rate v_P; an apparent kinetic is achieved. Therefore, we introduce the reduced polymerization rate v_E, the apparent encapsulation rate, which we define by the maximum deformation change over time (see Fig. 3a) by

$$-\frac{d[\mathrm{IC}]}{dt} = -\frac{d[\mathrm{AM}]}{dt} = v_P \sim v_E = -\frac{d(\delta_{max})}{dt} \tag{4}$$

We apply Equation 4 to determine the shape of the encapsulation rate law v_E which is given by

$$v_E = k_E \cdot [\mathrm{IC}]^{\alpha} \cdot [\mathrm{AM}]^{\beta} \tag{5}$$

Encapsulation rates v_E are determined from the slopes of the plots of δ_{max} over time at the initial stage ($d(\delta_{max})/dt$, see Fig. 3a). Reaction orders α and β are calculated from the slopes of the double logarithmic plots of v_E versus the concentration of the component that is varied at the experiments. The appropriate other reaction component concentrations are held constant at these experiments. Exemplary, the determination of the order referring to the

amine HMDA is shown in Figure 3b that yields 0.3. Figure 4 concludes determinations of orders referring to the isocyanate, the amines and surfactant Abil® EM 90.

We derive the W/O-encapsulation rate law that completely describes our system by

$$v_E = k_E^* \cdot [\mathrm{IC}] \cdot [\mathrm{AM}]^{0.3} \tag{6}$$

with

$$k_E^* = \frac{k_E}{[\mathrm{surfactant}]^{0.1}} \tag{7}$$

From this law we determine that an IC concentration increase by a factor of eight increases the total encapsulation rate v_E by eight and the equivalent increase in the AM concentration increases v_E solely by a factor of two. Hence, in the W/O system the amine that is located in the dispersed phase limits the overall encapsulation kinetics.

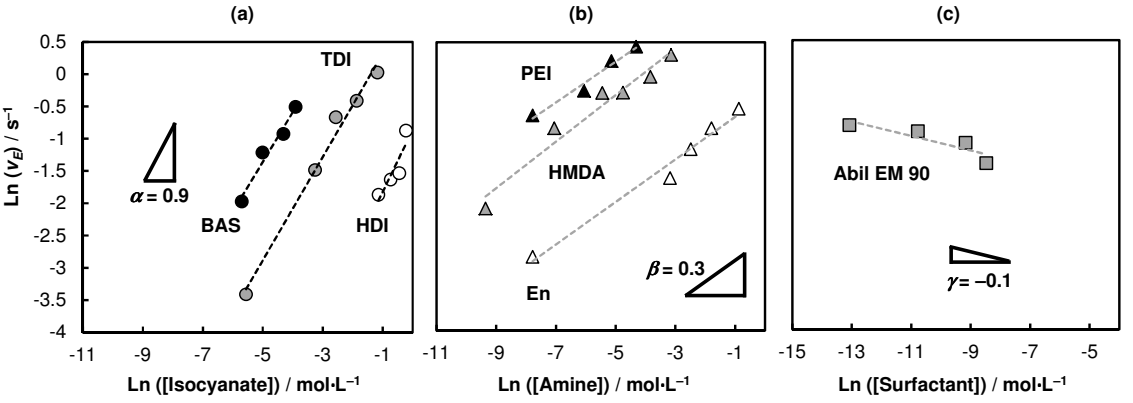

Fig. 4 Double-logarithmic plots of v_E versus the concentrations of the isocyanate (a), amine (b) and the surfactant (c) for the determination of orders α, β and γ. In detail: ▲ PEI (ln v_E = 0.28·ln [PEI] – 1.15), ▲ HMDA (ln v_E = 0.32·ln [HMDA] – 0.88), △ En (ln v_E = 0.30·ln [En] – 0.74); isocyanates are ● BAS (ln v_E = 0.77·ln [BAS] – 1.15), ● TDI (ln v_E = 0.80·ln [TDI] – 0.16). ○ HDI (ln v_E = 0.92·ln [HDI] – 2.02) and the surfactant Abil® EM 90 is ■ (ln v_E = –0.11·ln [ABIL] – 2.19).

Tab. 1 Relative encapsulation rate constants determined in this study and literature known reaction rate constants of conversions of *n*-butyl alcohol* with isocyanates and primary isocyanates with primary and secondary amines.[10,11]

Isocyanate	Amine	Relative Rate
TDI	En	1
	HMDA	4.98
	TEPA	5.99
	PEI	10.21
primary isocyanate	Secondary amine	1[10–11]
	Primary amine	2–5[10–11]
HDI	HMDA	1
BAS		6.52
TDI		9.07
HDI	*n*-butyl alcohol*	2, 1[10–11]**
TDI		792, 66.4[10–11]**
TDI	HMDA	1 (surfactant)
		4.98 (no surfactant)

*…There is no detailed information in literature available on the reaction rates of TDI and HDI with amines. The reaction of isocyanates with alcohols even though that it occurs slower than the reaction with amines by a factor of 100–1000 can be compared with the urea reaction and almost the same reactivity trends are found.

**… Values indicate the rate constant for converting the first and second isocyanate function, consecutively.

In Figure 4 for each plot of the isocyanates HDI, BAS and TDI we determine a slope of approximately 1 and for all amines we determine slopes around 0.3 which confirms the consistency of our hypothesis on v_E and the reproducibility of the experiments. We can now estimate the specific encapsulation rate constants for each component allowing for a detailed comparison of the monomer reactivities. Table 1 contains relative encapsulation rates of amines and isocyanates and literature known values of reaction rates of isocyanates with amines.[10,11]

The data particularly elucidate the reactivity differences of the molecules used in our investigations. Therefore, the aromatic isocyanate TDI has a 9-fold higher encapsulation rate than the aliphatic HDI. However, by considering literature known data of the pure conversion of these components we find that the reactivity difference between TDI and HDI are not exactly reflected in the changes of k_E. Obviously, the monomer diffusion throughout the interface limits the encapsulation rate. We remark another discrepancy when comparing the relative rates of different amines. The chemical structure of polyethyleneimine PEI exhibits a higher amount of secondary amines per mol than En and HMDA. However, the relative encapsulation rate of PEI is higher by a factor of 2–10 which is in contrast to the overall reactivity of secondary amines (Tab. 1). The authors assume that this effect is caused by an increased cross-linking tendency of PEI. The cross-linkage at the PEI/TDI reaction leads to a more drastic change in δ_{max} at the polymerization. As a consequence, capsules with strong networks that have a high elastic modulus result. In contrast, HMDA and En react with TDI to linear chains that form semi-crystalline structures with low elastic moduli. A similar trend is found for the isocyanate components (Tab. 1). The chemical reactivity of HDI and BAS are the same but the encapsulation rate v_E of BAS is higher than that of HDI by a factor of 7. BAS has 3 isocyanate functions which in combination with HMDA yields multiple cross-linked polymer networks with high elastic moduli. We see that the encapsulation rates v_E determined in our studies also reflect the changes in the morphology at the early stage of the shell formation (see also Eq. 3). However, its use is limited due to the fact that the capsule shell properties are currently unknown. A more detailed study on the shell properties by *ex situ* analysis of the capsules is subject of current studies in our lab.

In addition, we investigate the influence of the surfactant on the encapsulation kinetics. We use the polymeric surfactant Abil® EM 90 due to its suitable stabilization properties of aqueous drops in KMC oil. The surfactant has no direct influence on the chemical conversion, thus, in Equation 6 the rate constant k_E is replaced by k_E* (Eq. 7). In our range of surfactant concentrations the δ_{max} dynamics are not affected by the presence of the surfactant; the system already reached an equilibrium state. Reactions of the isocyanate with Abil® EM can be neglected. We find that the order referring to the surfactant is –0.1. Consequently, an increase of the surfactant amount causes a decrease in the overall encapsulation rate v_E. In addition, compared to the non-surfactant encapsulation (Tab. 1), the relative rate of the surfactant stabilized encapsulation is slower by a factor of five. The precise mechanism of the surfactant on the slowing down of the reaction is not known. Two mechanisms remain to explain the retardation. Firstly, it can be stated that the surfactant assembles at the W/O interface or it blocks reactive sites which reduces the probability for AM–IC impacts. Furthermore, it is known that the macroscopic structure of PUMCs is modified by the presence of surfactant.[13] The associated changes in the mechanical properties represented by the elastic modulus changes of the polymer network as described in [13] can be accounted for the slowdown dynamics.

4. Conclusion

The dynamics of the W/O-polyurea microcapsule formation were studied using microfluidic techniques. We visualized the encapsulation process by monitoring the deformability change of W/O emulsion droplets. Constant hydrodynamic shear stresses on the droplet – and capsules – were induced by microfluidic constriction chambers. We investigated the interfacial polyurea formation. We introduced the encapsulation rate law and the encapsulation rate v_E that is a measure for the change in the maximum deformation of the emulsion droplet over time while polymerizing. Based on this principle we showed that our approach enables for the precise measurements of

encapsulation kinetics (below 0.5 s with a resolution down to milliseconds) over a wide concentration range of the reactants (0.001–30 wt.%) with the potential of determining the interfacial polymerization kinetics. Both monomers contribute differently to the kinetics; for W/O polyurea microcapsules (PUMCs) the amine component which is located in the dispersed phase limits the encapsulation rate v_E. The PUMC encapsulation is retarded by a surface stabilizing agent (surfactant). The effect was quantified in this work applying the polymeric surfactant Abil® EM 90. We determined the order referring to the surfactant to be –0.1 indicating a decelerated diffusion of reactants throughout the W/O interface. Comparison of reactant reactivities revealed the dominating mechanistic steps at the encapsulation: the monomer diffusion throughout the membrane plays a crucial role at the encapsulation kinetics and an increased latent cross-linkage property of the monomers cause the formation of a rigid shell even at the early polymerization stage. Thereof, our microfluidic tool is tremendously practicable for monitoring encapsulation processes and it has the potential for a method to gain valuable insights into interfacial polymerization kinetics and the study of soft reactive interfaces as well as for the controlled production of shells along micro-compartments with adjustable membrane properties.

Acknowledgement

JCB acknowledges the financial support of the Max-Planck Society and the support by a funding from the European Research Council (ERC) under the European Union's Seventh Framework Program (FP7/2007-2013)/ERC Grant agreement 306385–Sofi.

References

1. Poshardi A, Kuna AJ, Microencapsulation Technology: A Review, *J. Res. Angrau* 2010; **38**: 86–10.
2. Benita S, *Microencapsulation Methods and Industrial Applications*, 2nd Ed. Taylor & Francis Group, Boca Raton, 2006.
3. Morgan PW, *Condensation Polymers: By Interfacial and Solution Methods*, John Wiley & Sons, New York, 1965.
4. MacRitchie F, Mechanism of Interfacial Polymerization, *Trans. Faraday Soc.* 1969, **65**: 2503–7.
5. Xia YN, Whitesides GM, *Abstr. Pap. Am. Chem. Soc.* 1997, **214**: 348.
6. Odian G, *Principles of Polymerization*, 4th Ed. John Wiley & Sons, Inc., Hoboken, New Jersey, 2004.
7. Brosseau Q, Vrignon J, Baret JC, Microfluidic Dynamic Interfacial Tensiometry (μDIT), *Soft Matter* 2014, **10**: 3066–76.
8. Taylor GI, The Formation of Emulsions in Definable Fields of Flow, *Proc. R. Soc. Lond. A* 1934, **146**: 501–23.
9. Cabral JT, Hudson SD, Microfluidic approach for rapid multicomponent interfacial tensiometry 2006, **6**: 427–36.
10. Delebecq E, Pascault JP, Boutevin B, Ganachaud F, On the Versatility of Urethane/Urea Bonds: Reversibility, Blocked Isocyanate, and Non-isocyanate Polyurethane, *Chem. Rev*. 2013, **113**: 80–118.
11. Entelis SG, Nesterov OV, Kinetics and Mechanism of the Reactions of Isocyanates with Compounds containing “Active” Hydrogen, *Rus. Chem. Rev*. 1966, **35**(12): 917–30.
12. [a] Liu KK, Williams DR, Briscoe BJ, Compressive deformation of a single microcapsule, *Phys. Rev. E* 1996, **54**: 6673–80. [b] Pozrikidis C, *Modeling and Simulation of Capsules and Biological Cells*, Chapman & Hall/CRC, London, 2003.
13. Polenz I, Weitz DA, Baret JC, Polyurea microcapsules in microfluidics: surfactant control of soft membranes, *Langmuir* 2014, DOI: 10.1021/la5040189.